

Forecasting the changes between endemic and epidemic phases of a contagious disease, with the example of COVID-19

JACQUES DEMONGEOT¹, PIERRE MAGAL^{2*}, AND KAYODE OSHNUBI¹

¹ AGEIS laboratory, UGA, 38700 La Tronche, France

² Univ. Bordeaux, IMB, UMR 5251, F-33400 Talence, France.

CNRS, IMB, UMR 5251, F-33400 Talence, France.

October 2, 2023

Abstract

Predicting the endemic/epidemic transition during the temporal evolution of a contagious disease.

Methods: Defining indicators for detecting the transition endemic/epidemic, with four scalars to be compared, calculated from the daily reported news cases: coefficient of variation, skewness, kurtosis, and entropy. The indicators selected are related to the shape of the empirical distribution of the new cases observed over 14 days. This duration has been chosen to smooth out the effect of weekends when fewer new cases are registered. For finding a forecasting variable, we have used the PCA (principal component analysis), whose first principal component (a linear combination of the selected indicators) explains a large part of the observed variance and can then be used as a predictor of the phenomenon studied (here the occurrence of an epidemic wave).

Results: A score has been built from the four proposed indicators using a Principal Component Analysis (PCA), which allows an acceptable level of forecasting performance by giving a realistic retro-predicted date for the rupture of the stationary endemic model corresponding to the entrance in the epidemic exponential growth phase. This score is applied to the retro-prediction of the limits of the different phases of the COVID-19 outbreak in successive endemic/epidemic transitions and three countries, France, India, and Japan.

Conclusion: We provided a new forecasting method for predicting an epidemic wave occurring after an endemic phase for a contagious disease.

*Corresponding author. e-mail: pierre.magal@u-bordeaux.fr

Keywords: *Contagious disease; Endemic phase; Epidemic wave; Endemic/epidemic transition forecasting; COVID-19 epidemic wave prediction*

The paper is dedicated to James D. Murray, whose pioneering work in mathematical biology we admire.

1 Introduction

Finding a reliable prediction method of the frontiers between different stationary and non-stationary periods of a time series is a challenging problem. Since the seminal work by Deshayes and Picard on the stationarity rupture in time series [1, 2, 3], many works have dealt with the break in stationarity [4, 5, 6, 7, 8, 9], the most recent using the concepts of functional statistics [10, 11, 12, 13, 14, 15, 16]. Indeed, stationarity is crucial as many forecasting models of time series rely on stationarity for easy modeling and obtaining reliable results. A stationary time series presents statistical properties which do not change over time, as the empirical distribution of the random variable observed in the series, with its main characteristic parameters, mean, coefficient of variation, moments, and entropy. In the event of a break in stationarity, there may be a sudden transition with a sudden change in the values of these parameters and the appearance of a non-constant trend. The problem of the existence of this transition arises with particular acuity in the case of contagious diseases, which alternate stationary endemic periods and epidemic peaks having an initial exponential trend, which must be predicted to prevent the spread of the disease does not give rise to a pandemic.

The term endemic phase is understood to mean a period in which there is an equilibrium in a model whose parameters have changed in value following an epidemic phase, due to mitigation measures or a change in the virulence of the infectious agent. In the case of chronic diseases observed outside epidemic phases (bacterial meningitis, rabies, smallpox before its eradication, etc.), the definition of endemicity corresponds more to the sporadic appearance (by birth or human displacement) of individuals much more susceptible than the general population to the infectious agent [17, 18, 19].

We will propose in this article a method to estimate the breakdown of endemic stationarity based on four parameters linked to the empirical distribution of the number of daily reported new cases of COVID-19 in several countries, parameters whose isolated or joint predictive power will be analyzed. These parameters are the coefficient of variation, the skewness, the kurtosis, and the entropy of the stationary empirical measure calculated in a moving window.

The pair represented by the succession of an endemic phase and an epidemic wave in COVID-19 outbreak can be considered as a functional unit, the break between the two phases having to be found [20, 21, 22, 23, 24, 25]. The endemic phase is characterized by a low average level of new cases, with low variance. At the start of the epidemic phase, the average number of cases will grow exponentially, and the standard deviation will grow proportionally at the beginning,

then saturate, like that of an additive noise in part independent of growth, which explains the increase then decrease in the coefficient of variation and kurtosis, therefore those of the first principal component at the endemic/epidemic boundary.

2 Materials and Methods

We use in the following a moving window of length 14 days for calculating the empirical distribution of the random variable equal to the number of daily reported new cases. The empirical distribution N_t on day t is obtained from the daily number of reported new cases considered as a random variable $N_t = (N(t-13), N(t-12), \dots, N(t))$.

The length of the window has been chosen for eliminating the effect of the week periodicity observed in data due to the lack of reporting each weekend. Indeed, daily new infection cases are highly affected by weekends, such that new case numbers are lowest at the start of the week, and increase afterwards [26].

2.1 Empirical first four moments

In the following we will use the terminology *endemic period*, to describe a period during which the daily new cases occurs randomly around some mean value. An *epidemic wave* is a period during which the daily new cases occurs by contact between susceptible and infected.

Our goal in this paper is to explore the transition between the endemic period and the following epidemic wave which will be studied by calculating several parameters in a moving window around the frontier of 14 days on which we suspect this transition occurred.

We consider the first four moments of N_t . We start with the *mean*

$$\mu = E(N_t) = \frac{\sum_{i=0}^{13} N(t-i)}{14}, \quad (2.1)$$

where E is the expectation operator, with the *standard deviation*

$$\sigma = E\left((N_t - \mu)^2\right)^{1/2} = \sqrt{\frac{\sum_{i=0}^{13} (N(t-i) - \mu)^2}{14}}. \quad (2.2)$$

From these two first parameters, we can compute the *coefficient of variation*

$$CV(N_t) = \frac{\sigma}{\mu}. \quad (2.3)$$

The *skewness* of the random variable N_t is the third standardized moment, defined as

$$Skew(N_t) = E \left(\left(\frac{N_t - \mu}{\sigma} \right)^3 \right). \quad (2.4)$$

Recall that the skewness verifies

$$Skew(N_t) = \frac{E(N_t^3) - 3\mu\sigma^2 - \mu^3}{\sigma^3} = \frac{E(N_t^3)}{\sigma^3} - \left(3\frac{1}{CV} + \frac{1}{CV^3} \right). \quad (2.5)$$

The *kurtosis* is the fourth standardized moment, defined as

$$Kurt(N_t) = E \left(\left(\frac{N_t - \mu}{\sigma} \right)^4 \right). \quad (2.6)$$

The *empirical entropy* \mathcal{E} of the empirical distribution is defined as follows:

$$\mathcal{E}(N_t) = - \sum_{i=1:d \text{ with } p_i > 0} p_i \log p_i, \quad (2.7)$$

where the p_i are the weights of a histogram on d value intervals of N_t . In the Results' section, we use the *approximate entropy*. We refer to [36] for more details.

2.2 Phenomenological model used for multiple epidemic waves

To represent the data, we used a phenomenological model to fit the curve of cumulative reported cases. Such an idea is not new since it was already proposed by Bernoulli [17] in 1760 in the context of the smallpox epidemic. Here we used the so-called Bernoulli–Verhulst [37] model to describe the epidemic phase. Bernoulli [17] investigated an epidemic phase followed by an endemic phase. This appears clearly in Figures 9 and 10 of the paper by Dietz, and Heesterbeek [38] who revisited the original article of Bernoulli. We also refer to Blower [18] for another article revisiting the original work of Bernoulli. Several works comparing cumulative reported cases data and the Bernoulli–Verhulst model appear in the literature (see [39, 40, 41]). The Bernoulli–Verhulst model is sometimes called Richard's model, although Richard's work came much later in 1959.

The phenomenological model deals with data series of new infectious cases decomposed into two successive phases: 1) endemic phases followed by 2) epidemic phases.

Endemic phase: During the endemic phase, the dynamics of new cases appears to fluctuate around an average value independently of the number of cases. Therefore the average cumulative number of cases is given by

$$CR(t) = N_0 + (t - t_0) \times a, \text{ for } t \in [t_0, t_1], \quad (2.8)$$

where t_0 denotes the beginning of the endemic phase, N_0 is the number of new cases at time t_0 , and a is the average value of the daily number of new cases.

We assume that the average daily number of new cases is constant. Therefore the daily number of new cases is given by

$$\text{CR}'(t) = a. \quad (2.9)$$

Epidemic phase: In the epidemic phase, the new cases are contributing to produce secondary cases. Therefore the daily number of new cases is no longer constant, but varies with time as follows

$$\text{CR}(t) = N_{\text{base}} + \frac{e^{\chi(t-t_0)} N_0}{\left[1 + \frac{N_0^\theta}{N_\infty^\theta} (e^{\chi\theta(t-t_0)} - 1)\right]^{1/\theta}}, \text{ for } t \in [t_0, t_1]. \quad (2.10)$$

In other words, the daily number of new cases follows the Bernoulli–Verhulst [17, 37] equation. Namely, by setting

$$N(t) = \text{CR}(t) - N_{\text{base}}, \quad (2.11)$$

we obtain

$$N'(t) = \chi N(t) \left[1 - \left(\frac{N(t)}{N_\infty}\right)^\theta\right], \quad (2.12)$$

completed with the initial value

$$N(t_0) = N_0.$$

In the model, $N_{\text{base}} + N_0$ corresponds to the value $\text{CR}(t_0)$ of the cumulative number of cases at time $t = t_0$. The parameter $N_\infty + N_{\text{base}}$ is the maximal value of the cumulative reported cases after the time $t = t_0$. $\chi > 0$ is a Malthusian growth parameter, and θ regulates the speed at which $\text{CR}(t)$ increases to $N_\infty + N_{\text{base}}$.

3 Results

Here we use cumulative numbers of reported new cases for COVID-19 in France, India, and Japan taken from WHO [42]. Data shows a succession of endemic periods (yellow background color regions) followed by epidemic waves (blue background color regions).

3.1 Data for France

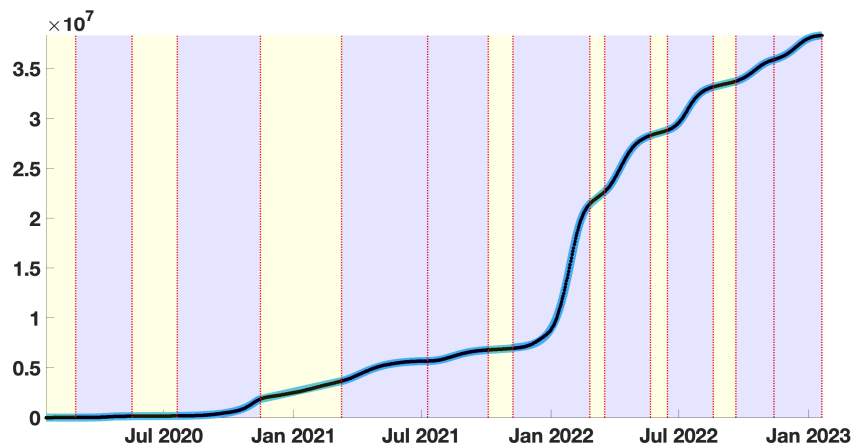


Figure 1: *In this figure we plot in blue the phenomenological model and in black the data. Data is the cumulative reported number of new cases with a 14-day rolling average.*

In Figure 2, each colored segment corresponds to a single endemic or epidemic phenomenological model. This change of color may occur due to a change of dynamic inside an epidemic phase when a second wave comes before the end of the previous one.

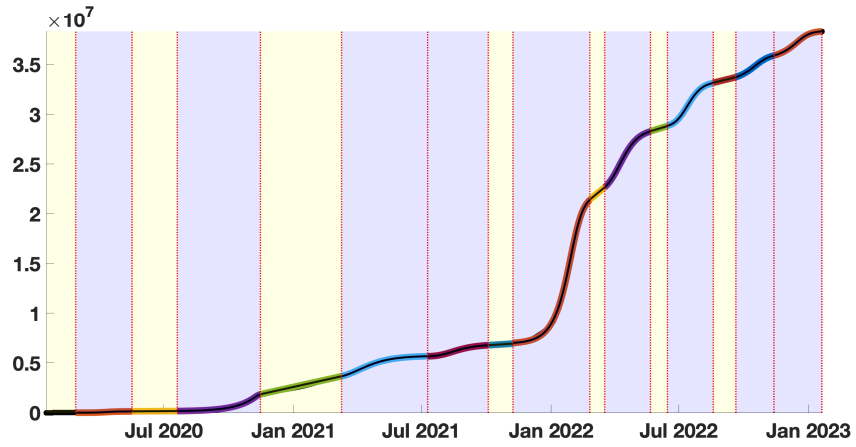


Figure 2: *In this figure we plot with multiple colors the phenomenological models obtained for each period.*

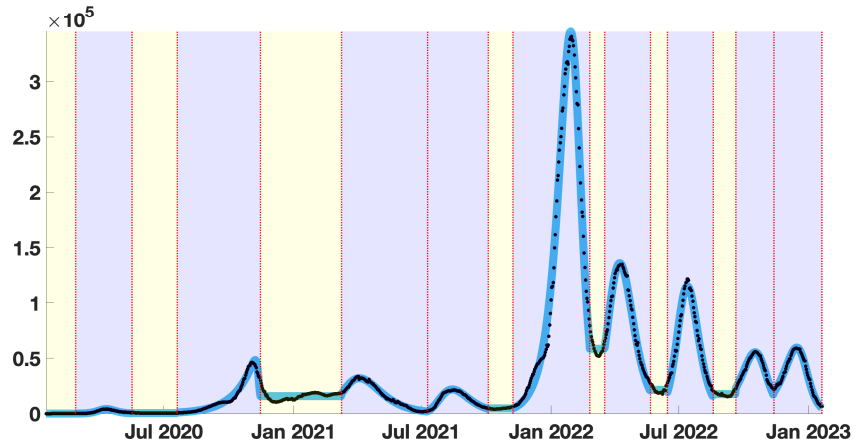


Figure 3: *In this figure we plot in blue the first derivative of the phenomenological model and in black the data. Data is the daily reported number of new cases with a 14-day rolling average.*

By making a principal component analysis (i.e. the matlab function PCA) between the standardized variables $CV_s(N_t)$, $Skew_s(N_t)$, $Kurt_s(N_t)$, $\mathcal{E}_s(N_t)$, we

obtain the percentage of the variance explained by each principal component

$$Explain = \begin{pmatrix} 70.71 \\ 21.92 \\ 4.94 \\ 2.43 \end{pmatrix}$$

and the matrix giving the projection coefficients of the principal components

$$coef = \begin{pmatrix} 0.5527 & -0.1480 & 0.7163 & -0.3995 \\ 0.5631 & -0.2162 & -0.0348 & 0.7968 \\ 0.5577 & -0.0795 & -0.6955 & -0.4461 \\ 0.2577 & 0.9618 & 0.0449 & 0.0808 \end{pmatrix}.$$

By using the first column of the above matrix, we deduce the first principal component

$$0.55CV_s(N_t) + 0.56Skew_s(N_t) + 0.56Kurt_s(N_t) + 0.26\mathcal{E}_s(N_t) \quad (3.1)$$

which explains 70.71% of the variability.

We deduce that Kurtosis, Skewness, and the coefficient of variation (in decreasing order of importance) best explain the variability.

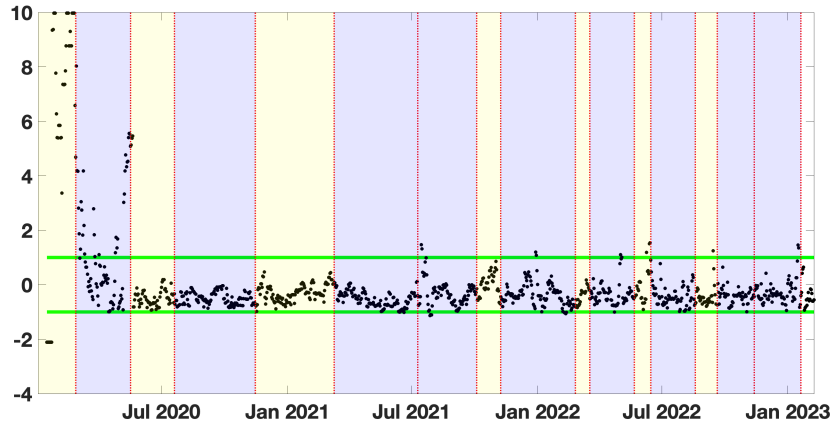


Figure 4: *In this figure we plot the first principal component for France (see formula (3.1)). The horizontal green lines correspond to ± 1 .*

3.2 Data for India

In this subsection, we consider the data for India. We present the same curves as for France, describing successively raw data and simulated results by the phenomenological models.

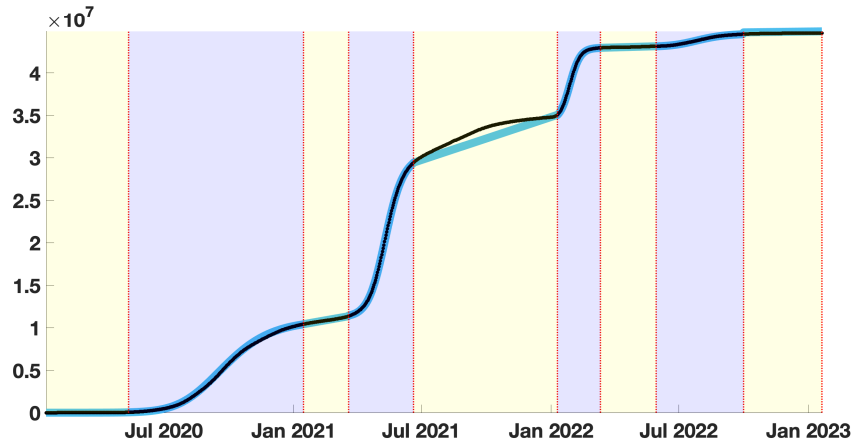


Figure 5: *In this figure we plot in blue the phenomenological model and in black the data. Data is the cumulative reported number of new cases with a 14-day rolling average.*

In Figure 6, each colored segment corresponds to a single endemic or epidemic phenomenological model. This change of color may occur due to a change of dynamic inside an epidemic phase when a second wave comes before the end of the previous one.

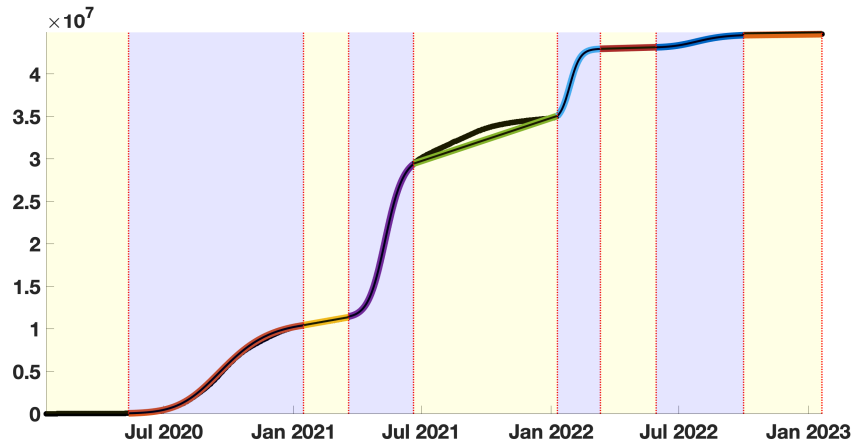


Figure 6: *In this figure we plot with multiple colors the phenomenological models obtained for each period.*

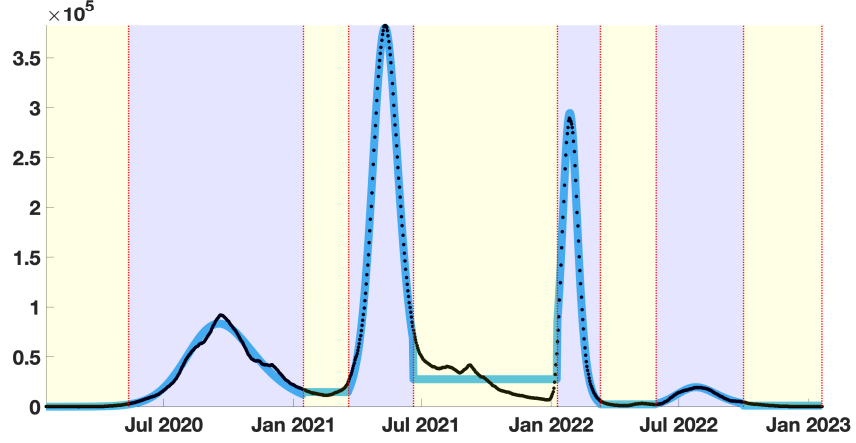


Figure 7: In this figure we plot in blue the first derivative of the phenomenological model and in black the data. Data is the daily reported number of new cases with a 14-day rolling average.

By making a principal component analysis (i.e. the matlab function PCA) between the standardized variables $CV_s(N_t)$, $Skew_s(N_t)$, $Kurt_s(N_t)$, and $\mathcal{E}_s(N_t)$, we obtain the percentage of the variance explained by each principal component

$$Explain = \begin{pmatrix} 53.13 \\ 22.55 \\ 14.22 \\ 10.09 \end{pmatrix}$$

and the matrix giving the projection coefficients of the principal components

$$coeff = \begin{pmatrix} 0.5161 & -0.2296 & 0.8212 & -0.0810 \\ 0.5714 & -0.0587 & -0.4434 & -0.6881 \\ 0.5660 & -0.2235 & -0.3478 & 0.7133 \\ 0.2946 & 0.9455 & 0.0896 & 0.1062 \end{pmatrix}.$$

By using the first column of the above matrix, we deduce the first principal component

$$0.52CV_s(N_t) + 0.57Skew_s(N_t) + 0.57Kurt_s(N_t) + 0.29\mathcal{E}_s(N_t) \quad (3.2)$$

which explains 53% of the variability.

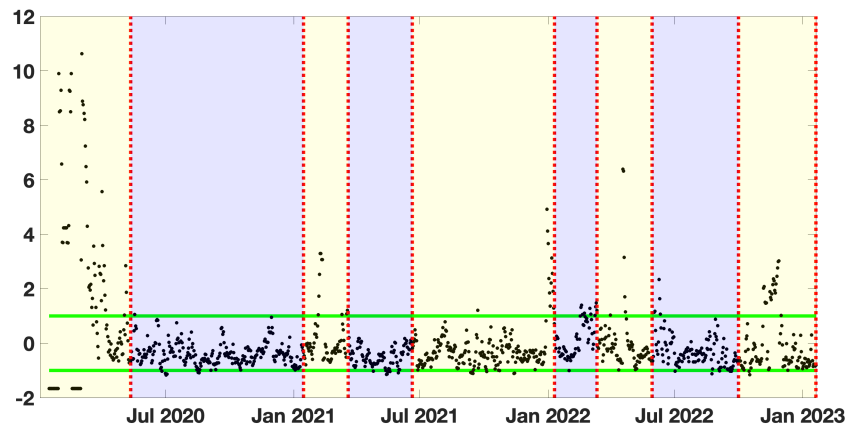


Figure 8: *In this figure we plot the first principal component for India (see formula (3.2)). The horizontal green lines correspond to the values ± 1 .*

3.3 Data for Japan

In this subsection, we consider the data for Japan. We present the same curves as for France and India, describing successively raw data and simulated results by the phenomenological models.

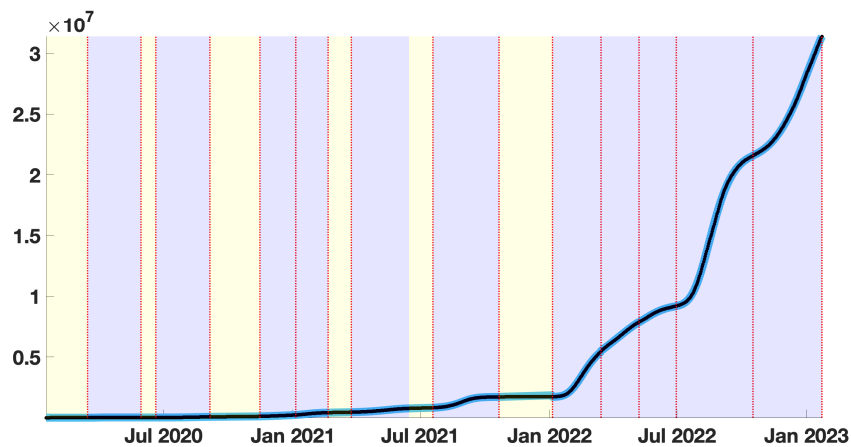


Figure 9: *In this figure we plot in blue the phenomenological model and in black the data. Data is the cumulative reported number of new cases with a 14-day rolling average.*

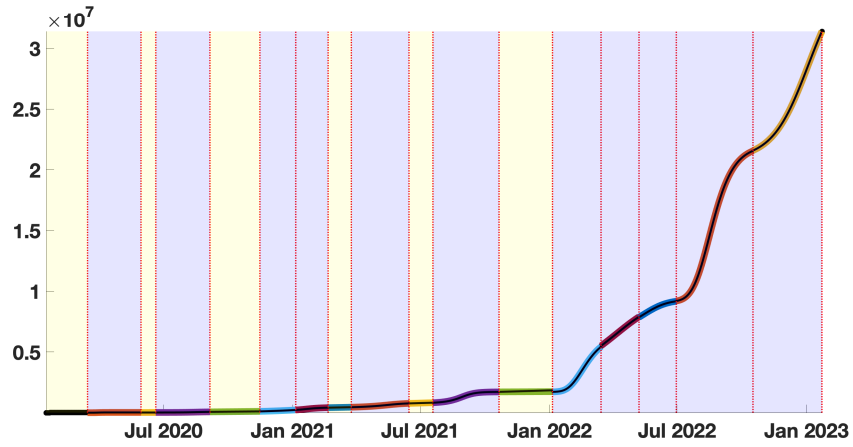


Figure 10: *In this figure we plot with multiple colors the phenomenological models obtained for each period.*

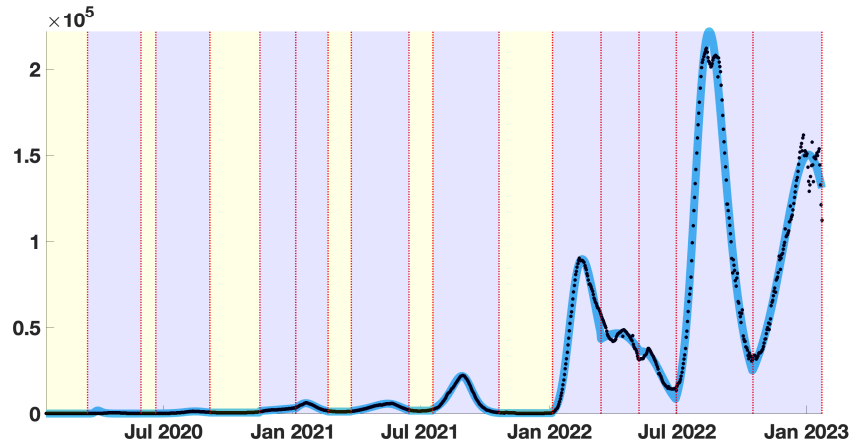


Figure 11: *In this figure we plot in blue the first derivative of the phenomenological model and in black the data. Data is the daily reported number of new cases with a 14-day rolling average.*

By making a principal component analysis (i.e. the matlab function PCA) between the standardized variables $CV_s(N_t)$, $Skew_s(N_t)$, $Kurt_s(N_t)$, and $\mathcal{E}_s(N_t)$,

we obtain the percentage of the variance explained by each principal component

$$Explain = \begin{pmatrix} 71.62 \\ 17.54 \\ 6.87 \\ 3.97 \end{pmatrix}$$

and the matrix giving the projection coefficients of the principal components

$$coef = \begin{pmatrix} 0.5234 & -0.2243 & 0.7969 & -0.2018 \\ 0.5452 & -0.2406 & -0.2310 & 0.7691 \\ 0.5401 & -0.1760 & -0.5575 & -0.6054 \\ 0.3703 & 0.9278 & 0.0270 & 0.0358 \end{pmatrix}.$$

By using the first column of the above matrix, we deduce the first principal component

$$0.52CV_s(N_t) + 0.55Skew_s(N_t) + 0.54Kurt_s(N_t) + 0.37\mathcal{E}_s(N_t) \quad (3.3)$$

which explains 71% of the variability.

We deduce that Kurtosis, Skewness, and the coefficient of variation (in decreasing order of importance) best explain the variability.

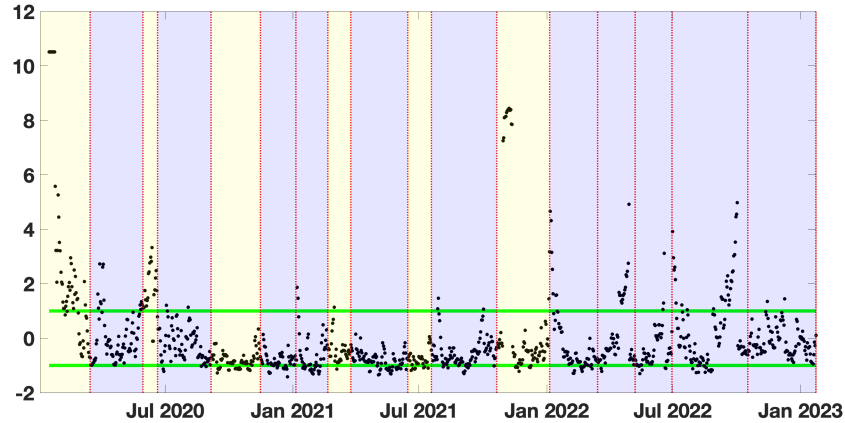


Figure 12: *In this figure we plot the first principal component for Japan (see formula (3.3)). The horizontal green lines correspond to the values ± 1 .*

4 Discussion

The forecasting of the epidemic waves of the COVID-19 outbreak is based on a change in the nature of the time series dynamics related to the number of

daily new reported cases of this contagious disease. This change can concern the moments or the entropy of the empirical distribution of the stationary component at the end of the endemic phase, which disrupts when a not constant trend occurs, marking the start of an epidemic wave.

From a careful examination of Figures 4, 8 and 12, we can conclude that there are not constant but frequent patterns for $C_1(t)$ identifiable in the three studied countries and for a majority of their endemic/epidemic transitions.

The predictive power of the first principal component $C_1(t)$ can be quantified by its performance ratio, that is, by the percentage of correct retro-predictions obtained by fixing variation thresholds to forecast the occurrence of an epidemic wave. For France, if we fix the threshold to the value 1, $C_1(t)$ predicts correctly an epidemic outbreak a week after a decrease from this threshold value not reached elsewhere in the endemic phase. This prediction is correct at 53% only for India. For Japan, the performance of the retro-prediction is 71% and 70% for France.

It is clear that the level of prediction is not very high (71% in the best case), but, in the absence of a currently reliable predictor, we can consider that it is sufficient to trigger mitigation measures at level of a population. A more systematic study of the changing shape of the empirical distribution is needed, looking at many epidemic waves in many countries. A parameter measuring the deviation from classical laws (such as those linked to the Kolmogorov-Smirnov, chi-square or Shapiro-Wilk tests in the case of the normal law) could thus be added in subsequent works.

As previously noticed in [43], a classical epidemic peak with a near-symmetric growth and decline may be preceded or followed by a shoulder-like behavior corresponding to a prematurely stopped wave followed by another. Shoulder-like behavior for epidemic waves can be explained by using multiple sub-group epidemic models. This idea was first explored for SARS-CoV-1 in [44] and reconsidered for SARS-CoV-2 by [45]. But the changes between endemic and epidemic are still challenging to model.

5 Conclusions

We have studied in this article the evolution of four parameters related to the dynamics of the number of the daily reported new cases N_t at day t of a contagious disease, which can serve as early indicators of the appearance of epidemic waves from a previous endemic state. By applying this parameter calculation to COVID-19, we showed that a score obtained by PCA based on the linear combination of the four chosen parameters with specific coefficients for each one could forecast the variations of the empirical distribution of the daily reported number of new cases N_t , then could be considered often as a good predictor (for the countries and the epidemic waves in these countries) of the endemic-epidemic transition. A systematic study of contagious diseases other than COVID-19 is necessary to confirm this forecasting property's existence. Still, we can already propose this score as a realistic indicator of the next occurrence of an epidemic

outbreak from a change in the dynamics of the observed daily new cases during the endemic periods.

References

- [1] Deshayes, J., & Picard, D. Application aux tests de rupture de régression. *Astérisque* 1979, 68, 73-98.
- [2] Deshayes, J., & Picard, D. Lois asymptotiques des tests et estimateurs de rupture dans un modèle statistique classique. *Annales de l'I.H.P. Probabilités et statistiques* 1984, 20, 309-327.
- [3] Picard, D. Testing and estimating change-points in time series. *Advances in applied probability*, 1985, 17(4), 841-867.
- [4] Vogt, M., & Dette, H. Detecting gradual changes in locally stationary processes. *The Annals of Statistics* 2015, 43, 713-740.
- [5] van Delft, A., & Eichler, M. Locally stationary functional time series. *Electronic Journal of Statistics* 2018, 12, 107-170.
- [6] Palachy, S. Detecting stationarity in time series data. *Medium Towards Data Sci.* (2019), 9, 53.
- [7] Ting, K.M., Liu, Z., Zhang, H., & Zhu, Y. A new distributional treatment for time series and an anomaly detection investigation. *Proceedings of the VLDB Endowment* (2022), 15, 2321-2333.
- [8] Hauber, A.L., Sigloch, C., & Timmer, J. Detecting frequency modulation in stochastic time-series data. *Physical Review E* (2022), 106, 024204.
- [9] Bawdekar, A.A., Prusty, B.R., & Bingi, K. Sensitivity Analysis of Stationarity Tests' Outcome to Time Series Facets and Test Parameters. *Mathematical Problems in Engineering* 2022, 2022, 2402989.
- [10] Demongeot, J., Laksaci, A., Madani, F., & Rachdi, M. Functional data: local linear estimation of the conditional density and its application. *Statistics* (2013), 47, 26-44.
- [11] Rachdi, M., Laksaci, A., Demongeot, J., Abdali, A., & Madani, F. Theoretical and practical aspects on the quadratic error in the local linear estimation of the conditional density for functional data. *Comp. Stat. Data Anal.* (2014), 73, 53-68.
- [12] Demongeot, J., Laksaci, A., Rachdi, M., & Rahmani, S. On the local linear modelization of the conditional distribution for functional data. *Sankhya A* (2014), 76, 328-355.

- [13] Demongeot, J., Hamie, A., Laksaci, A., & Rachdi, M. Relative-Error Prediction in Nonparametric Functional Statistics: Theory and Practice. *Journal of Multivariate Analysis* (2016), 146, 261-268.
- [14] Belkis, A., Demongeot, J., Laksaci, A., & Rachdi, M. Functional data analysis: Estimation of the relative error in functional re-gression under random left-truncation. *J. Nonparametric Statistics* (2018), 30, 472-490.
- [15] Oshinubi, K., Ibrahim, F., Rachdi, M., & Demongeot, J. Functional Data Analysis: Application to Daily Observation of COVID-19 Prevalence in France. *AIMS Mathematics* (2022), 7, 5347-5385.
- [16] Jelassi, M., Oshinubi, K., Rachdi, M., & Demongeot, J. Epidemic Dynamics on Social Interaction Networks. *AIMS Bioengineering* (2022), 9, 348-361.
- [17] Bernoulli, D. Essai d'une nouvelle analyse de la petite Vérole, & des avantages de l'Inoculation pour la prévenir, *Mémoire Académie Royale des Sciences, Paris*, 1760.
- [18] Blower S, & Bernoulli D. An attempt at a new analysis of the mortality caused by smallpox and of the advantages of inoculation to prevent it. (1766). *Rev Med Virol.* (2004) Sep-Oct;14(5):275-88.
- [19] Murray J.D., Stanley E.A., Brown D.L. On the spatial spread of rabies among foxes. *Proc R Soc Lond B Biol Sci.* (1986) Nov 22;229 (1255):111-50.
- [20] Cinaglia, P., & Cannataro, M. Forecasting COVID-19 epidemic trends by combining a neural network with R_t estimation. *Entropy* (2022), 24(7), 929.
- [21] Srivastava, S. R., Meena, Y. K., & Singh, G. Forecasting on Covid-19 infection waves using a rough set filter driven moving average models. *Appl. Soft. Comput.* (2022) Dec;131:109750.
- [22] Lynch, C. J., & Gore, R. Short-range forecasting of COVID-19 during early onset at county, health district, and state geographic levels using seven methods: comparative forecasting study. *Journal of medical Internet research*, 23(3) (2021), e24925.
- [23] Lynch C.J., & Gore R. Application of one-, three-, and seven-day forecasts during early onset on the COVID-19 epidemic dataset using moving average, autoregressive, autoregressive moving average, autoregressive integrated moving average, and naïve forecasting methods. *Data Brief.* (2021) Apr;35:106759.
- [24] Yu CS, Chang SS, Chang TH, Wu JL, Lin YJ, Chien HF, & Chen RJ. A COVID-19 Pandemic Artificial Intelligence-Based System With Deep

Learning Forecasting and Automatic Statistical Data Acquisition: Development and Implementation Study. *J Med Internet Res.* (2021) May 20;23(5):e27806.

- [25] ArunKumar KE, Kalaga DV, Sai Kumar CM, Chilkoor G, Kawaji M, & Brenza TM. Forecasting the dynamics of cumulative COVID-19 cases (confirmed, recovered and deaths) for top-16 countries using statistical machine learning models: Auto-Regressive Integrated Moving Average (ARIMA) and Seasonal Auto-Regressive Integrated Moving Average (SARIMA). *Appl Soft Comput.* 2021 May;103:107161.
- [26] Demongeot, J., Oshinubi, K., Rachdi, M., Seligmann, H., Thuderoz, F., & Waku, J. Estimation of daily reproduction rates in COVID-19 outbreak, *Computation*, 9, 109 (2021).
- [27] Demongeot, J., & Magal, P. Spectral method in epidemic time series. *Biology* (2022), 11, 1825.
- [28] Worldometer. Available online: <https://www.worldometers.info/coronavirus> (Accessed on 6 January 2023).
- [29] Caswell, H. *Matrix population models: construction, analysis and interpretation*, 2nd ed. Sinauer: Sunderland, (2001).
- [30] Demongeot, J., & Demetrius, L. Complexity and Stability in Biological Systems. *Int. J. Bifurcation and Chaos* (2015), 25, 40013.
- [31] Nicol-Harper, A., Dooley, C., Packman, D., Mueller, M., Bijak, J., Hodgson, D., Townley, S., & Ezard, T. Inferring transient dynamics of human populations from matrix non-normality. *Popul Ecol.* (2018), 60, 185-196.
- [32] Xu, Z., Yang, D., Wang, J., & Demongeot, J. Statistical Analysis Supports UTR (untranslated region) Deletion Theory in SARS-CoV-2. *Virulence* (2022), 13, 1772-1789.
- [33] Demongeot, J., Griette, Q., Maday, Y., & Magal, P. A Kermack-McKendrick model with age of infection starting from a single or multiple cohorts of infected patients. *Proc. Royal Society A* (2023), 479, 2022.0381.
- [34] Kammegne, B., Oshinubi, K., Babasola, T., Peter, O.J., Longe, O.B., Ogunrinde, R.B., Titiloye, E.O., & Demongeot, J. Mathematical modelling of spatial distribution of COVID-19 outbreak using diffusion equation. *Pathogens* (2023), 12, 88.
- [35] Xu, Z., Wei, D., Zeng, Q., Zhang, H., Sun, Y., & Demongeot, J. More or less deadly? A mathematical model that predicts 1 SARS-CoV-2 evolutionary direction. *Computers in Biology & Medicine* 2023, 153, 106510.
- [36] Pincus, S. M. Approximate entropy as a measure of system complexity. *Proceedings of the National Academy of Sciences*, 88(6) (1991), 2297-2301.

- [37] Verhulst, P. F. Notice sur la loi que la population poursuit dans son accroissement, *Corresp. Mathématique Phys.*, (1938),113-121.
- [38] Dietz, K., & Heesterbeek, J. A. P. Daniel Bernoulli's epidemiological model revisited, *Math. Biosci.*, 180 (2002), 1-21.
- [39] Hsieh, Y. H. Richards model: a simple procedure for real-time prediction of outbreak severity, in *Modeling and dynamics of infectious diseases*, (2009), 216–236.
- [40] Wang, X.S., Wu, J., & Yang, Y. Richards model revisited: validation by and application to infection dynamics, *J. Theoret. Biol.*, 313 (2012), 12-19.
- [41] Zhou, G., & Yan, G. Severe acute respiratory syndrome epidemic in Asia, *Emerg. Infect. Dis.*, 9 (2003), 1608-1610.
- [42] Data from WHO. Accessed: July 20, 2022. <https://COVID19.who.int/WHO-COVID-19-global-data.csv>
- [43] Weitz, J. S., Park, S. W., Eksin, C., & Dushoff, J. Awareness-driven behavior changes can shift the shape of epidemics away from peaks and toward plateaus, shoulders, and oscillations. *Proceedings of the National Academy of Sciences*, 117(51) (2020), 32764-32771.
- [44] Magal, P., Seydi, O., & Webb, G. Final size of a multi-group SIR epidemic model: Irreducible and non-irreducible modes of transmission. *Mathematical biosciences*, 301 (2018), 59-67.
- [45] Chowell, G., Dahal, S., Tariq, A., Roosa, K., Hyman, J. M., & Luo, R. An ensemble n-sub-epidemic modeling framework for short-term forecasting epidemic trajectories: Application to the COVID-19 pandemic in the USA. *PLoS Computational Biology*, 18(10) (2022), e1010602.